

AUTOMATIC BREAK-LINE DETECTION FROM LASER SCANNER DATA USING SURFACE FLATNESS

H. YOKOYAMA^a, H. CHIKATSU^a

^a Tokyo Denki Univ., Dept. of Civil Eng., Hatoyama, Saitama, 350-0394 JAPAN
E-mail: yokoyama@chikatsu-lab.g.dendai.ac.jp , chikatsu@g.dendai.ac.jp

Commission V, WG V/4

KEY WORDS: Spatial Information Sciences, Automation, Cultural Heritage, Extraction, Laser scanning, Three-dimensional

ABSTRACT:

Recently, a laser scanner has been receiving more attention as a useful tool for real-time 3D data acquisition, and various applications such as city modelling, DTM generation and 3D modelling of cultural heritage were proposed. However, robust filtering for distinguish on- and off-terrain points from point cloud 3D data collected by airborne laser scanner is still issues.

In particular, filtering of point cloud 3D data collected by terrestrial laser scanner has more severe problems caused by many occlusion parts, windows, few the deepest points, wall of buildings and so on. With this motive, robust filtering and break-line detection method using surface flatness was developed by the authors in 2004.

However, the method needs any manual setting. This issue becomes a particularly serious problem in break-line detection for various objects. In order to perform manual setting for break-line detection, automatic break-line detection method by using variation of flatness will be described in this paper.

1. INTRODUCTION

With respect to recording work, it is essential to reduce the amount of time, labor, and skill employed while making archival records of a historical structure.

In order to do so a laser scanner is used to measure the sites, and on the basis of the results, a break-line is detected.

A break-line is extracted as a characteristic part such as an edge of stack or a corner of building by a laser scanner measurement result (Point Cloud Data).

In the surveying field, examination of the break-line extraction method which was used LIDAR data is performed. In the case of the LIDAR data, measurement is performed only from the sky. Data processing is examined variation of height course. Furthermore, the automatic extracting methods of break-line are examined with variation of height course. As one method, the method using open angle of topography is examined. However, threshold value is set with experience.

In 2005, the filtering method using surface flatness for terrestrial laser scanner was suggested. This method revises a facial direction with normal vector. Therefore, the same standard evaluation is enabled. However, the threshold value of break-line extraction was determined by manual operation. Break-line of the site where small shape variation and intense shape variation coexist cannot extract by one threshold.

In this paper, the automation technique of threshold value setting for the filtering was discussed. Break-line extraction method for the area where small shape variation and intense shape variation coexist was examined in same time.

2. WORK FLOW OF FILTERING AND BREAK-LINE EXTRACTION

Figure1 shows work flow of break-line extraction.

Recently, the laser scanner has attracted considerable attention as measurement tool that can perform extensive 3D measurements in real time. A Total Station is used for this purpose in same purpose, but it requires a greater amount of labour and skill.

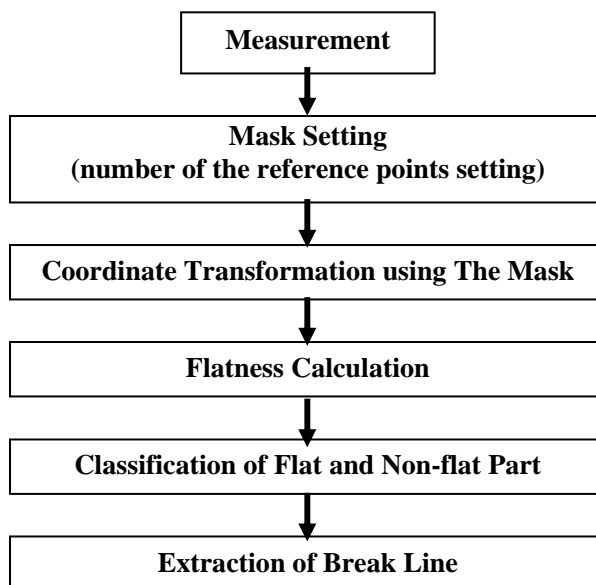


Fig.1 Work Flow of Break-line Extraction

So, the authors measured the historical structure and carried out recording using laser scanners for labour saving by work flow of Fig.1.

About recording method for characteristic part of historical structure, efficient break-line method for 3D point cloud data was introduced. This paper describes about automatic setting of the threshold for 3D point cloud data.

3. CLASSIFICATION OF THE FLAT AND NON-FLAT AREAS IN CUSTOMARY METHOD

Break-lines are included in boundary of flat and non-flat part. Therefore, Classification of the flat and non-flat area is necessary before break-line extraction.

In order to classified of flat and non-flat area, 3D point cloud data was acquired using terrestrial laser scanner. A small mask with 30*30 cm area is used instead of the 3D information samples. After a 3*3 point mask is generated around an interest point, the mask size expands to 30*30 cm by computing the plane coordinates for the neighbor points. The mask is then transformed so that in the first step, a normal vector for the mask becomes parallel to the Z-axis (Figure 2). In the next step, the standard deviation (S.D.) is computed for the interest point. The threshold value should be considered while classifying the interest points into flat (ground surface, structure walls, etc.) and non-flat areas (trees, bushes, sky, etc.). The threshold value is determined on the basis of the measured data. Figure3 shows the Measurement targets for reference of S.D. and figure4 shows the S.D. values with some mask sizes.

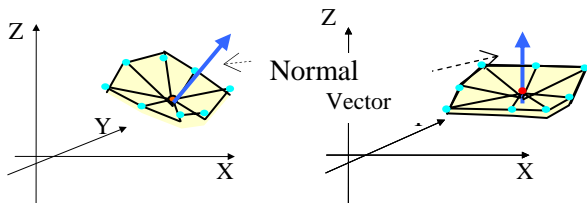


Fig.2 Coordinate Transformation Image

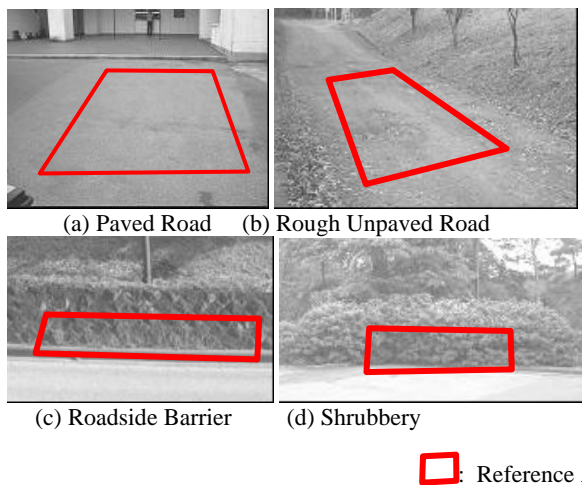


Fig.3 The Measurement Targets for Reference.

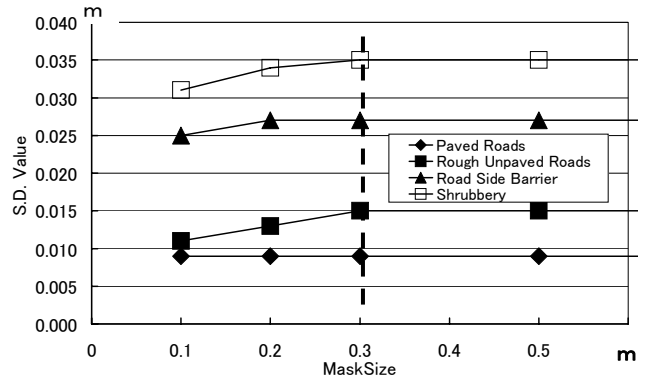


Fig.4 S.D. Values for Some Mask Sizes

4. AUTOMATION OF BREAK-LINE EXTRACTION

By customary method, the mask size was fixed to 0.3*0.3m. However, in cases for small shape such as relief, current mask size is too big. Furthermore, as for the thresholds to separate flat and non-flat part was set by manual. The thresholds were based on reference results, and thresholds were coordinated. The coordinated work was done repeatedly. Therefore automation of setting was demanded.

4.1 Mask Sizing in New Method

If mask size has enough size, flatness is stable in figure 4. Stability of mask size is different by reference target. The stable size was searched by chasing variation of flatness. Equation 1 was used for the chasing.

$$f(r) = \frac{(r^2)^{1/2}}{2\pi\sigma^4} \exp\left\{-\frac{r^2}{2\sigma^2}\right\} \quad (1)$$

where,
 $r := (\sqrt{x^2 + y^2})^{1/2}$, σ : standard deviation,
 (x,y) : Position from notice point

This equation is the Gaussian function with second expression. The Gaussian function is known as smooth a minute data variation. This equation can be utilised to detect inflection point of data in automatic. Figure 5 shows the sample data of S.D. values for some mask sizes and inflection point

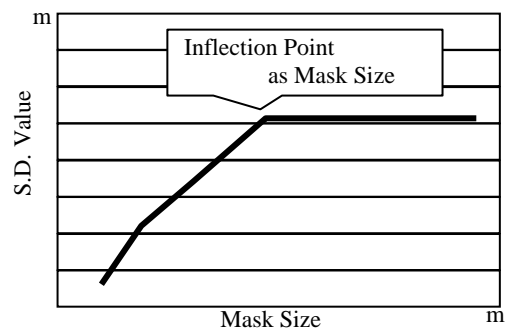


Fig.5 sample data of S.D. values for some mask sizes and inflection point

4.2 Automation of Thresholds Setting

After a mask size was decided, coordinate transformation using normal vector is done. Threshold is set by manual operation, and notice point is classified by flat part and non-flat part.

Figure 6 are range image and intensity image of the castle wall, and they were used for flatness evaluation in this paper.

Range image is the image which showed in difference of color with distance from laser scanner to measuring points. Intensity image shows in difference of color with intensity reflection of laser.



(a) Range Image

(b) Intensity Image

Fig.6 Range Image and Intensity Image



(c)Target

Fig.6 Range Image and Intensity Image

Figure 7 shows the histogram which calculated flatness about all measuring point. About creation of histogram, standard deviation (S.D.) of flatness was demanded, and the histogram separated range of $3 \times \text{S.D.}$ to 256th grade. Figure 8 shows flatness value image. Brightness value of this image is the same setting of histogram.

Figure 9 is the intensity image which showed with black in the part considered to be non-flat part. With a depth map, distinction of flat is difficult. Therefore the figure uses intensity image.

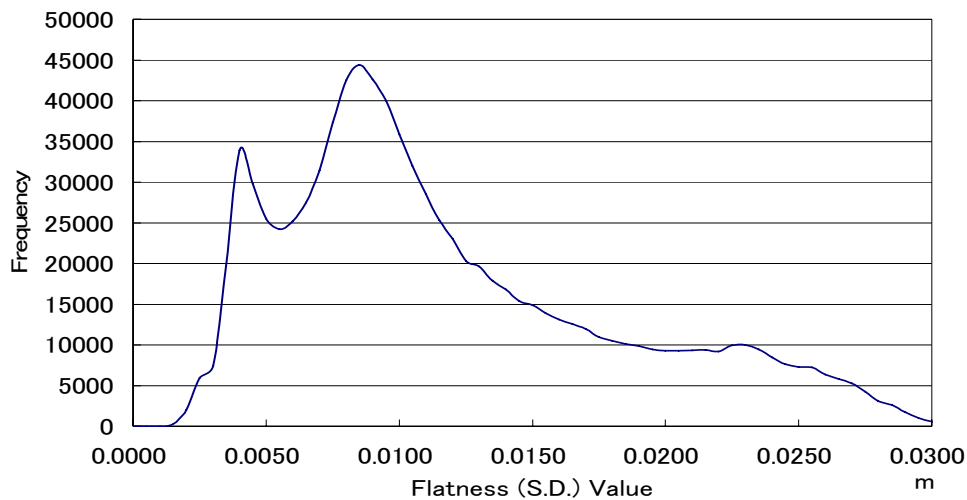


Fig.7 Histogram of Flatness (S.D.) Value

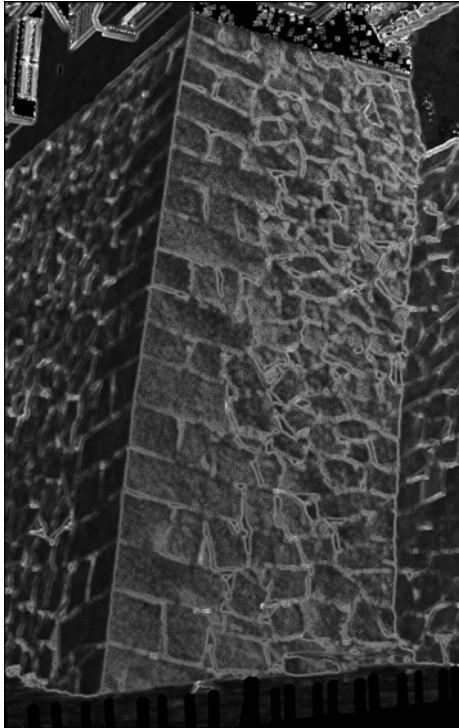
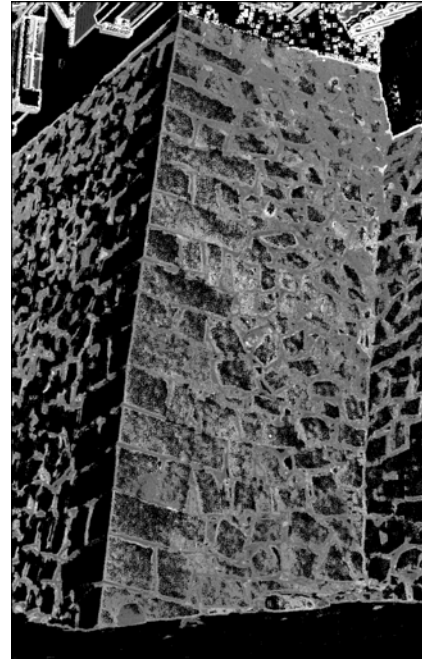


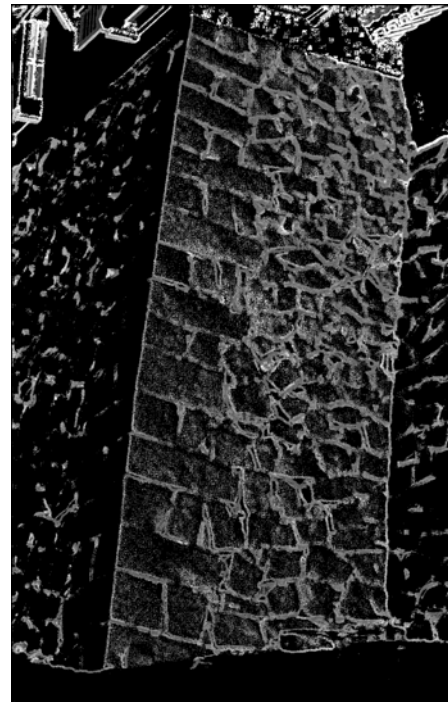
Fig.8 Flatness Value Image



(b) Threshold=0.005m



(a) Threshold=0.005m
Fig.9 Classified Result by Flatness



(c) Threshold=0.012m
Fig.9 Classified Result by Flatness

The stone wall to show for figure 6 extracts break-lines in corner and gap part are desired. Furthermore, break-lines are included in non-flat part. When histogram set the highest flatness in thresholds, the best result is provided in figure8 (Except the case that flatness is zero.).

Therefore, threshold setting is automated because histogram sets the highest flatness in thresholds except the case that flatness becomes zero.

4.3 Several Threshold Setting

Incidentally, break-lines are extracted from irregularity part. In other words, in the site where flat shape and complicated shape coexist, a break line is extracted by both shapes. Threshold to separate in flat and non-flat part is set with histogram of flatness shown to figure 7.

Therefore frequency of histogram is smaller than the first threshold, but it is point having enough frequency. In addition, flatness of neighbouring points are classified as flat part. Such a point was classified as non-flat part.

At first, mask is set around notice point to set threshold. The mask size is the size which was used by calculation of flatness. Average of flatness with point in mask is requested in afterwards.

Flatness to be next to the frequency which was used for threshold in the histogram is found.

The flatness will be considered to the second threshold. Flatness of notice point is higher than threshold, and the average of the points is lower than threshold is classified for non-flat part.

4.4 Break line Extraction

A break line is included in non-flat, and it will be peak value in neighbouring point. Figure 9 shows situation of break-line in non-flat part.

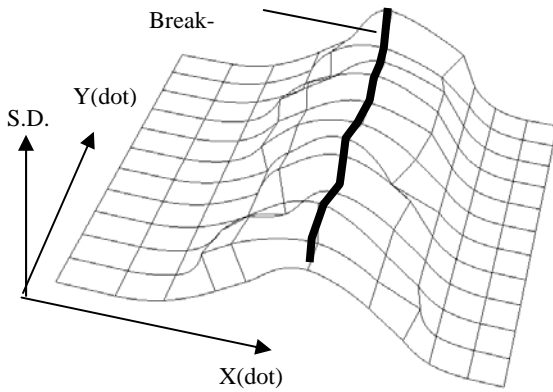


Fig.9 Situation of Break-line in Non-flat Part

A break line is extracted by finding peak of flatness. Furthermore, a break line is extracted efficiently by considering directionality of a break line. Therefore the following equation was used to examine directionality of a break line. This equation can calculate a direction of an edge of a peak.

$$\theta(x, y) = \arctan(h_y(x, y)/h_x(x, y)) \quad (2)$$

Where,

$\theta(x, y)$: Direction angle of peak value

$$h_x(x, y) = \int_{-\pi}^{\pi} \int_0^{\infty} f(x + r \cos \theta, y + r \sin \theta) - \frac{r \cos \theta}{2\sigma^2} \exp\left(-\frac{r^2}{2\sigma^2}\right) dr d\theta$$

$$h_y(x, y) = \int_{-\pi}^{\pi} \int_0^{\infty} f(x + r \cos \theta, y + r \sin \theta) - \frac{r \sin \theta}{2\sigma^2} \exp\left(-\frac{r^2}{2\sigma^2}\right) dr d\theta$$

$r := (x^2 + y^2)^{1/2}$, σ : standard deviation,
(x,y): Position of notice point

After a direction of a break line was confirmed, change of flatness is examined about vertical direction of a confirmed direction. To find peak of the change, equation (1) which was used for mask size setting is used. When the notice point was judged to be peak of change, the point classified as break line.

5. BREAK-LINE EXTRACTED RESULT

Figure 10 is the break-line extracted result. By figure 9, one threshold was set. In the break-line extraction result in figure 9, partial break-lines are not extracted, or unnecessary break-lines were extracted.

On the other hand, result of figure 11 sets two threshold. As a result, fine break-line was provided in comparison with figure 9.

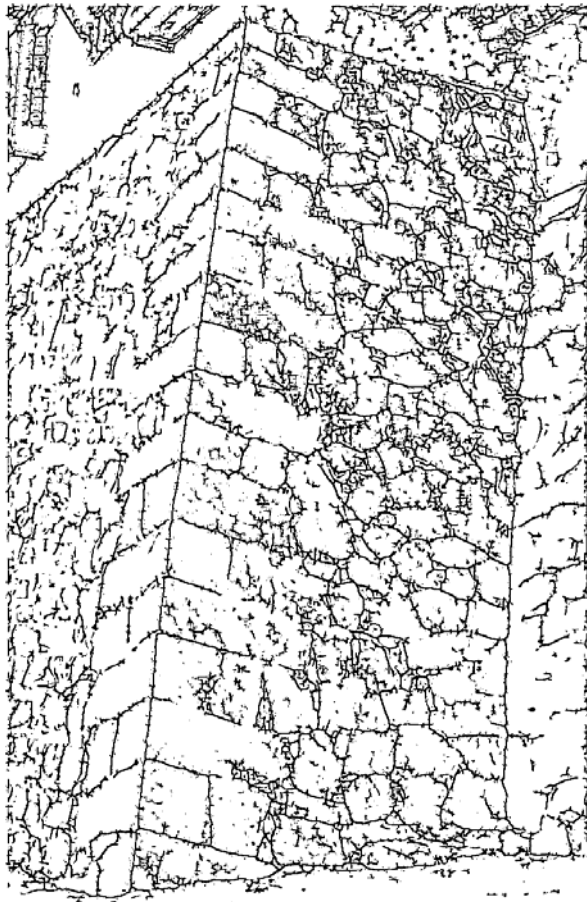


(a) Result of Single Threshold (S.D.=0.005 m)

Fig.10 Break-line Extracted Result



(b) Result of Single Threshold (S.D.=0.012 m)

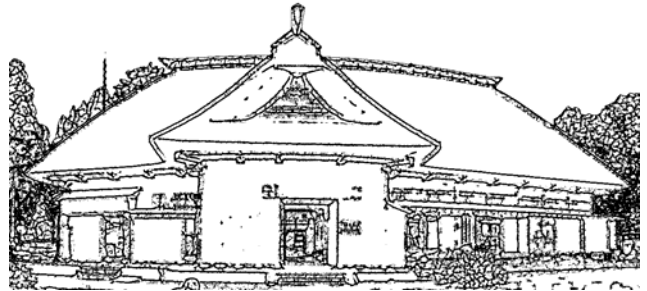


(c) Result of New Method
Fig.10 Break-line Extracted Result

As the reason that a good result was provided, several threshold has been set. By some threshold setting, fine break-lines were extracted in the site where different flatness coexisted. Figure11 is the break-line extracted result by another target. As a result, validity of this method was confirmed too.



(a) Target (Historical Structure)



(b) Break-line Extracted Result

Fig.11 Break-line Extracted Result (Historical Structure)

6. CONCLUSION

The most remarkable points as results of this approach are its ability to threshold setting of automatic break-line extract.

As for further additional results of this investigation, utility of break-line to other targets can be archived. Therefore, we'll continue examination about automatic unification method of coordinate systems and effective modelling method.

REFERENCES

- 1.Brugelmann, R., 2000. Automatic breakline Detection from sairborne Laser Range Data. IAPRS, Vol.XXXIII, Part B3, Amsterdam, The Netherlands, pp. 109-116.
- 2.H.YOKOYAMA, H. CHIKATSU,2004,Efficient Corner Detector for 3D point Crowd Data and application to 3D modeling of Structures,Proceedings of Electric Imaging Science and Technology "Videometrics VIII", Vol.5013, pp.208-215
- 3.T.SUGIYAMA, K.ABE, 1995. Edge height and reliability, Proc. ACCV '95, Singapore, Vol.II,pp.410-414
- 4.Wild, D., Krzystek, P., Madani, M., 1996, Automatic breakline detection using an edge preserving filter, IAPRS, 31, B3, pp. 946-952
5. D.GENELETTI, B.G.H. GORTE, 2003, A method for object-oriented land cover classification combining Lasndsat TM data and aerial photographs, ISPRS Journal of Photogrammetry and Remote Sensing, 24,6, pp. 1273-1286